

Electron energy enhancement by frequency chirp of a radially polarized laser pulse during ionization of low-density gases

This content has been downloaded from IOPscience. Please scroll down to see the full text.

2016 Plasma Phys. Control. Fusion 58 115011

(<http://iopscience.iop.org/0741-3335/58/11/115011>)

View [the table of contents for this issue](#), or go to the [journal homepage](#) for more

Download details:

IP Address: 198.125.232.28

This content was downloaded on 05/10/2016 at 21:01

Please note that [terms and conditions apply](#).

Electron energy enhancement by frequency chirp of a radially polarized laser pulse during ionization of low-density gases

Kunwar Pal Singh^{1,2}, Rashmi Arya², Anil K Malik^{3,4} and N J Fisch⁵

¹ Singh Simutech Pvt Ltd, Bharatpur, Rajasthan-321201, India

² Department of Physics, Shri Venkateshwara University, Gajraula, Amroha, UP-244236, India

³ Institute of Optics, University of Rochester, Rochester, NY 14627, USA

⁴ Department of Physics, Multanmodal Modi College Modinagar, CCS University, Meerut, UP-201204, India

⁵ Department of Astrophysical Sciences, Princeton University, Princeton, NJ 08540, USA

E-mail: k_psingh@yahoo.com

Received 14 June 2016, revised 10 August 2016

Accepted for publication 31 August 2016

Published 3 October 2016



Abstract

A scheme is proposed to enhance the energy of the electrons generated during the ionization of low-density krypton ions Kr^{32+} and argon ions Ar^{16+} by a radially polarized laser pulse using a negative frequency chirp. If a suitable frequency chirp is introduced then the energy of the electrons increases significantly and scattering decreases. The optimum value of the frequency chirp decreases with laser intensity and as well as spot size. The laser spot size also has an optimum value. The electron energy shows strong initial phase dependence. The scheme can be used to obtain quasi-monoenergetic collimated MeV/GeV electrons using the right choice of parameters. The chirped radially polarized laser pulse is more efficient than a chirped circularly polarized laser pulse to enhance energy and obtain quasi-monoenergetic electron beams.

Keywords: laser, acceleration, ionization, plasma

(Some figures may appear in colour only in the online journal)

Introduction

With the development of the chirped-pulse amplification technique [1, 2], table-top high-peak-power lasers have been successfully developed with light intensities as high as $10^{21} \text{ W cm}^{-2}$, which has generated great interest in laser-plasma-based accelerators. There have been a series of experimental achievements leading to the production of quasi-monoenergetic electron beams with energies in the range of 100 MeV to 1 GeV [3–5]. Particle accelerators find applications in x-ray lasers [6], laser-plasma-based harmonic generation [7], laser-driven inertial confinement fusion [8], high-resolution radiography for nondestructive material inspection, comprehensive zero-jitter pump-probe analysis, radiotherapy, ultrafast chemistry, femtosecond time-scale measurements, radiobiology and material science.

Energy enhancement by frequency chirp of linearly and circularly polarized laser pulses has attracted great interest in recent years. The interaction of free charged particles with a chirped electromagnetic pulse was investigated and it was found that, in contrast to the case of an unchirped pulse, the charged particle energy can be changed after the interaction [9]. Electron energy enhancement was proposed using a frequency chirp for a short, intense, linearly polarized focused laser pulse in a vacuum [10]. A scheme for electron acceleration by two crossing chirped lasers was proposed and important effects of the frequency chirp of the laser on electron acceleration were reported [11]. Electron acceleration by a chirped Gaussian laser pulse was investigated numerically using a linear and negative chirp for a linearly polarized laser pulse [12]. Gupta *et al* [13] commented on the results in [12] and showed that the electron obtains higher acceleration with

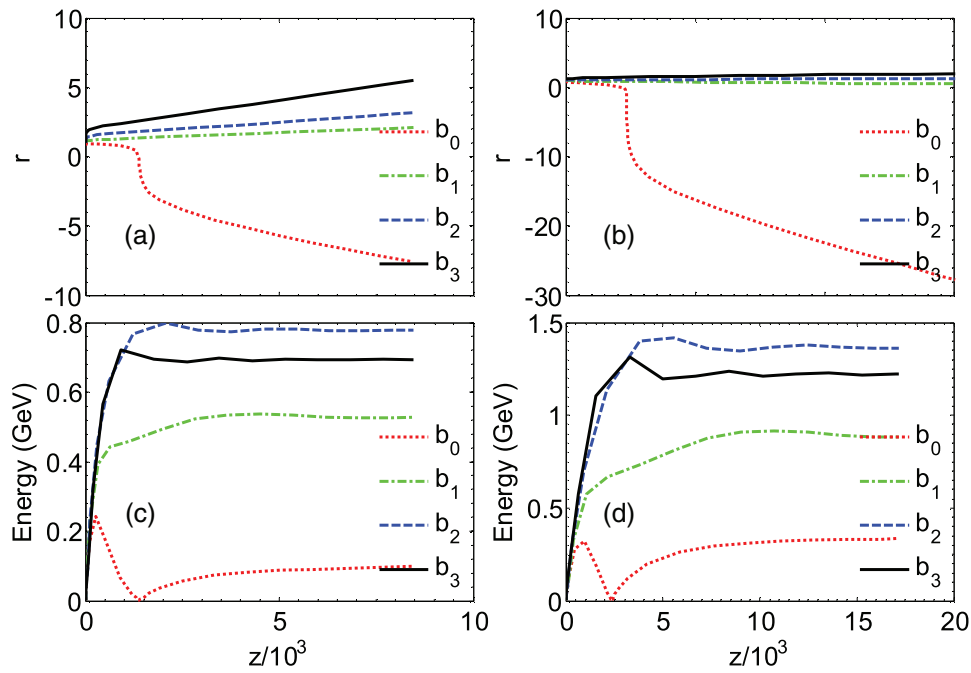


Figure 1. Electron trajectory in the $r - z$ plane and electron energy as a function of z for $a_0 = 50$. The initial position of the electron is at $r_i = 1$ and $z_0 = 0$. The normalized laser spot size $r_0 = 25$ in parts (a) and (c) and $r_0 = 50$ in parts (b) and (d). The different colored lines represent laser frequency chirp parameters $b_0 = 0$, $b_1 = 3.57 \times 10^{-6}$, $b_2 = 7.1 \times 10^{-6}$, and $b_3 = 1.1 \times 10^{-5}$ for parts (a) and (c) and $b_0 = 0$, $b_1 = 1.55 \times 10^{-6}$, $b_2 = 3.1 \times 10^{-6}$, and $b_3 = 4.66 \times 10^{-5}$ for parts (b) and (d).

a circularly polarized chirped laser pulse than with a linearly polarized chirped laser pulse. The combined effect of tight focusing and frequency chirping of the linearly polarized laser pulse on the acceleration of an electron in a vacuum was investigated [14]. Quasi-monoenergetic electrons from the ionization of a gas by a circularly polarized chirped intense laser pulse were investigated [15]. Electron acceleration was studied using a linearly and negatively chirped Gaussian beam in paraxial approximation and expressions for spot size, radius of curvature, and Rayleigh length were obtained [16]. Electron acceleration induced by a tightly focused linearly polarized chirped laser pulse in vacuum was investigated using fifth-order correction description [17]. The peculiarities of the laser phase behavior associated with the accelerated electron under the influence of a chirped laser pulse were qualitatively analyzed [18]. Electron acceleration by laser in a vacuum by a quadratically chirped laser pulse was investigated and it was found that the maximum energy gain is about half of what it would be using a linear chirp [19]. Obtaining monoenergetic collimated electron beams with increased energy is a challenge in the field [5]. Electron energy enhancement by frequency chirp of a radially polarized laser pulse during ionization of low-density gases has not been studied until now. In this paper, we show that the energy of the electron can be enhanced and scattering can be suppressed using a chirped radially polarized laser pulse.

Electromagnetic fields and electron dynamics

A radially polarized laser pulse [20] with an initial peak position z_L , pulse duration τ , and spot size r_0 , propagates along the z -axis towards the atoms assumed ahead of the laser pulse at

z_i, r_i . The electrons are generated with zero initial momentum during ionization and accelerated to high energy. For the ions, we have assumed that the outer electrons have been removed by a prepulse as described in [21]. We have assumed that the gas density/pressure is low enough to neglect plasma effects such as wakefield generation, magnetic field generation, focusing/defocusing, filamentation, etc [22]. A negative frequency chirp given by $\omega_0/(1 + bt)$ has been used, where ω_0 is the laser frequency without any chirp, b is the chirp parameter, and t is time. We examined a positive frequency chirp and determined that it produces lower energy than a negative frequency chirp so we have focused on negative frequency chirps only.

The normalized laser intensity parameter is given by $a_0 = eE_0/m_0\omega c$, $a_r = eE_r/m_0\omega c$, $a_z = eE_z/m_0\omega c$, and the normalized magnetic field is given by $b_{r,\theta,z} = eB_{r,\theta,z}/m_0\omega$, where $-e$ and m_0 are electron charge and rest mass, respectively. Throughout this paper time, length, and velocity are normalized by $1/\omega$, $1/k$, and c , respectively.

The equations governing electron momentum are obtained from the relativistic Newton–Lorentz equation of motion and solved numerically by a 2D acceleration simulation code to obtain the electron trajectory and momentum. For complete details of the model, please see [23].

Results and discussion

In this section, we describe the results of our simulations and discuss their implications. The fixed parameters are the normalized pulse duration $\tau = 200$ and initial position of laser pulse peak $z_L = -300$ for figures 1–3 and $z_L = -700$ for figures 4–7.

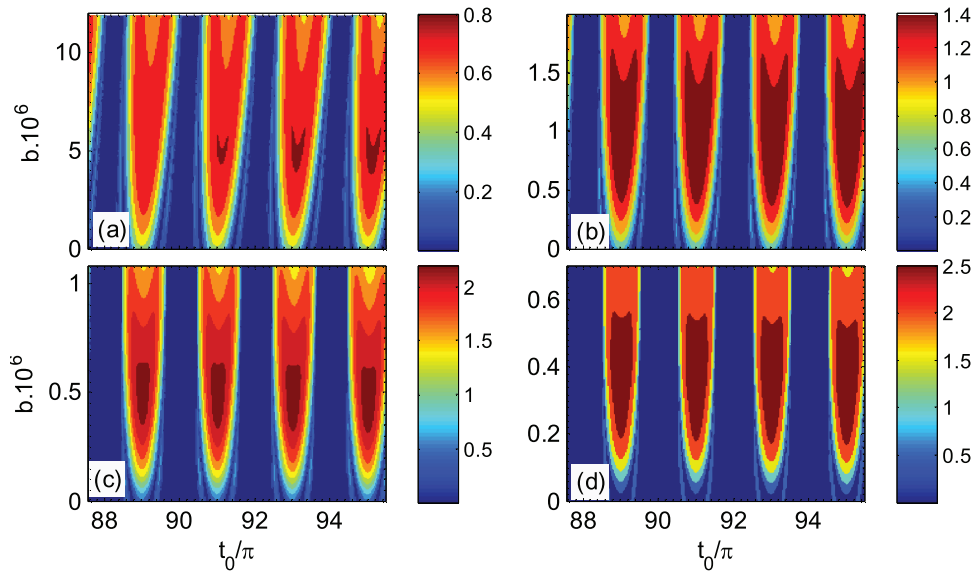


Figure 2. Distribution of electron energy (in GeV) as a function of normalized initial time t_0 and frequency chirp parameter b for normalized laser intensity parameter $a_0 = 50$, initial position of the electron at origin ($z_0 = r_i = 0$) and normalized laser spot size (a) $r_0 = 25$, (b) $r_0 = 50$, (c) $r_0 = 75$, and (d) $r_0 = 100$.

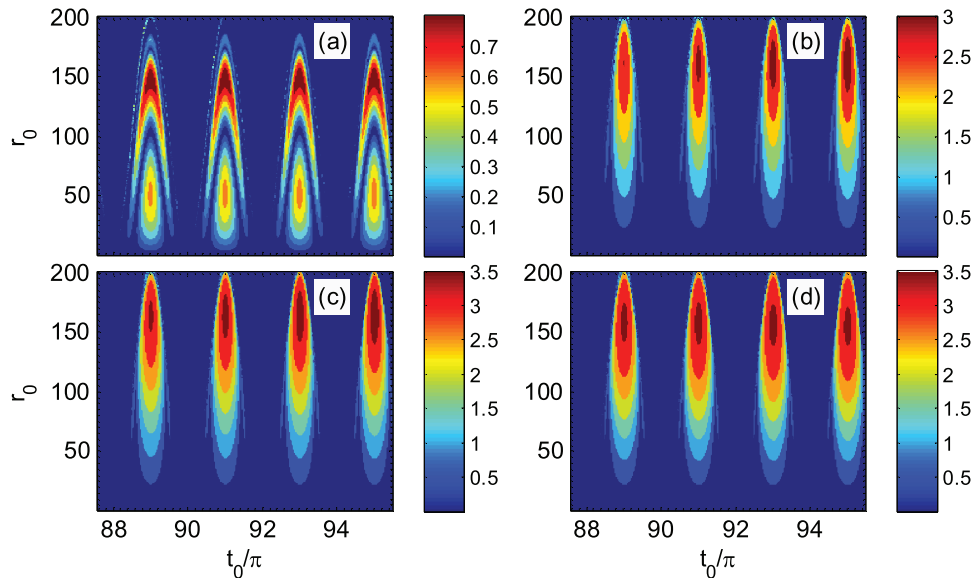


Figure 3. Distribution of electron energy (in GeV) as a function of normalized time t_0 and normalized laser spot size r_0 for normalized laser intensity parameter $a_0 = 50$, initial position of the electron at origin ($z_0 = r_i = 0$), and frequency chirp parameters (a) $b = 0$, (b) $b = 3 \times 10^{-7}$, (c) $b = 4 \times 10^{-7}$, and (d) $b = 5 \times 10^{-7}$.

Figures 1(a) and (b) show the trajectory of the electron in the $r - z$ plane for $r_0 = 25$ and $r_0 = 50$, respectively, for $a_0 = 50$. Figures 1(c) and (d) show the corresponding energy (in GeV) as a function of z . The initial position of the electron is at $r_i = 1$ and $z_0 = 0$. It can be seen from figure 1 that the electron trajectory is modified by the frequency chirp. Without the frequency chirp, the electron escapes from the pulse sooner, reducing the interaction duration, and consequently the electron energy decreases. With the introduction of the frequency chirp, the trajectory of the electron is modified in such a way that the electron interacts with the laser pulse for a longer duration and gains more energy. There is an approximately 6–8 times enhancement in the energy of the test electron with the introduction of the frequency chirp. It

can also be seen from the figures that the energy gain peaks for an optimum value of frequency chirp. The frequency chirp introduces asymmetry in the shape of the laser pulse. If the interaction duration is too short, the electron escapes from the pulse without getting sufficient time to gain energy, and if the interaction duration is too long, the electron can lose energy interacting with the trailing part of the laser pulse; therefore, there exists an optimum value of the frequency chirp. The optimum value of the frequency chirp is only approximately 2.5% for $r_0 = 25$ at energy saturation time.

Figures 2(a)–(d) show the electron energy for different values of normalized laser spot sizes $r_0 = 25$, $r_0 = 50$, $r_0 = 75$, and $r_0 = 100$, respectively. It can be seen that the electron energy shows a strong dependence on the electron

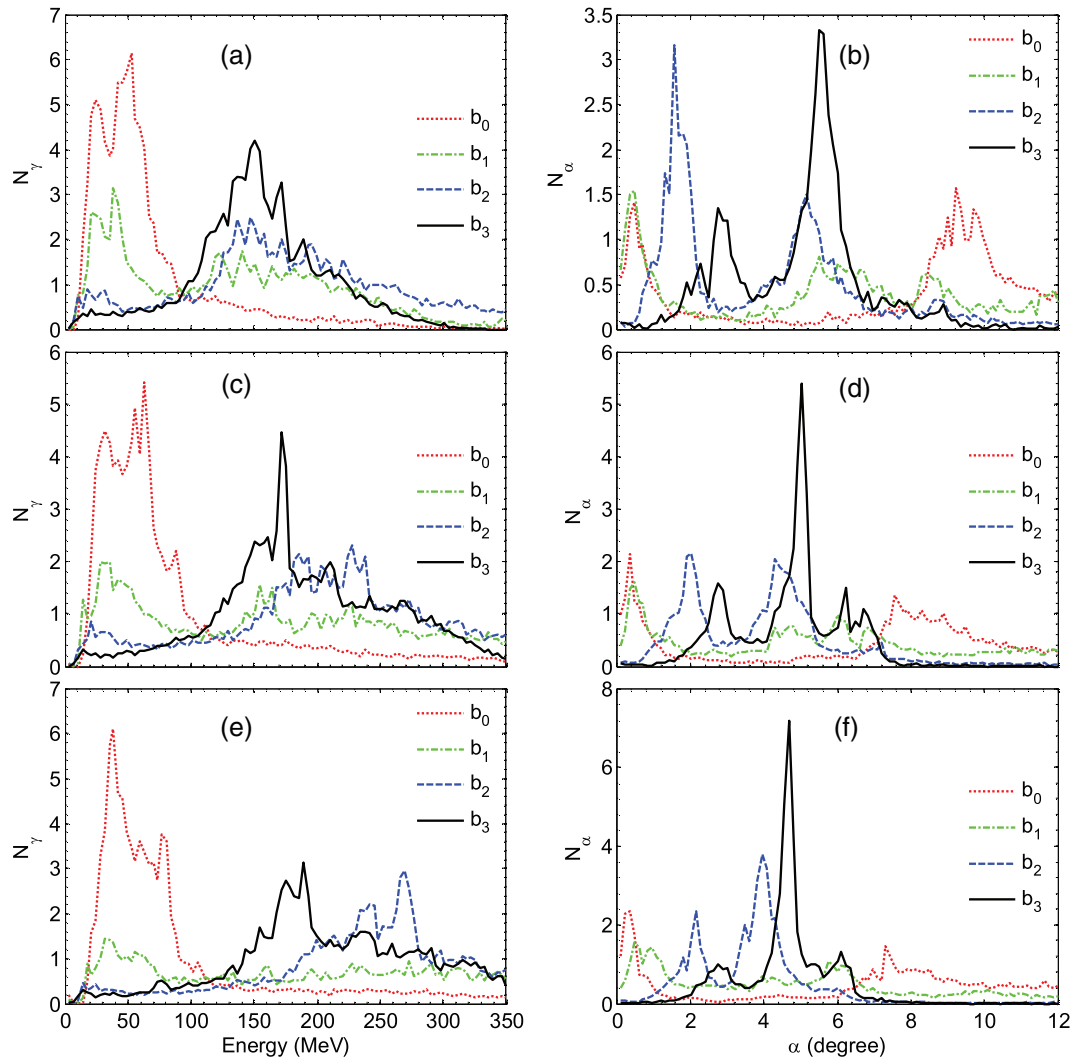


Figure 4. Spectrum of (a), (c), (e) energy and (b), (d), (f) angle of emittance of the electrons generated during ionization of krypton ions Kr^{32+} by a radially polarized laser pulse. The laser intensity parameters are $a_0 = 40, 50,$ and 60 for parts (a)–(f), respectively. The different colored lines are for laser frequency chirp parameters $b_0 = 0, b_1 = 10^{-4}/a_0^{0.5}, b_2 = 2 \times 10^{-4}/a_0^{0.5},$ and $b_3 = 3 \times 10^{-4}/a_0^{0.5}$.

generation time t_0 , or equivalently it can be said that it shows strong phase dependence. The energy is at its maximum when t_0 is an odd multiple of π and it is at its minimum when t_0 is an even multiple of π . The electron energy is maximum for an optimum value of frequency chirp parameter b . The optimum value of the frequency chirp parameter b decreases with increasing normalized laser spot size. The optimum value of the frequency chirp can be approximated by $7.5 \times 10^{-4}/r_0^{1.5}$ for the particular parameters for this figure. The energy distribution is not symmetric around electron generation time t_0 for normalized laser spot size $r_0 = 25$ in figure 2(a). This may be due to more asymmetry introduced by the frequency chirp at small values of laser spot size.

The distribution of electron energy as a function of normalized initial time t_0 and normalized laser spot size r_0 is shown in figure 3 for frequency chirp parameters $b = 0, b = 3 \times 10^{-7}, b = 4 \times 10^{-7},$ and $b = 5 \times 10^{-7}$. It can be seen from figure 3(a) (without any frequency chirp) that energy is at its maximum for a normalized laser spot size around $r_0 = 140$ ($r_0 = 2.8a_0$) and the secondary maximum of energy is around $r_0 = 50$ ($r_0 = a_0$). With the introduction of a frequency chirp,

the energy maximum shifts to a higher value of normalized laser spot size $r_0 = 165$ ($r_0 = 3.3a_0$) and the secondary maximum disappears. It can also be noted that there is approximately a 4.0–4.5 times enhancement in the energy with the introduction of the frequency chirp.

The energy requirement increases with laser spot size; therefore, we have chosen a small value of laser spot size $r_0 = a_0$ for figures 4–7 in the following description.

The last normalized time is 10^6 for figures 4–7. We have taken krypton ions Kr^{32+} and argon ions Ar^{16+} randomly distributed from $r = -r_0$ to r_0 and $z_0 = 0$ to 100 to generate approximately 1 million electrons for the results of figures 4–7. The N_γ and N_α are obtained by dividing the whole range of energy and angle of emittance into 100 parts and then counting the number of electrons (relative scale) with energy lying within a range of relativistic factor, and scattering angle lying within a range of angle of emittance, respectively, for figures 4 and 5 in the following description [23].

We will now discuss the acceleration of electrons generated during the ionization of krypton ions Kr^{32+} . The spectrum of energy and angle of emittance of the electrons generated

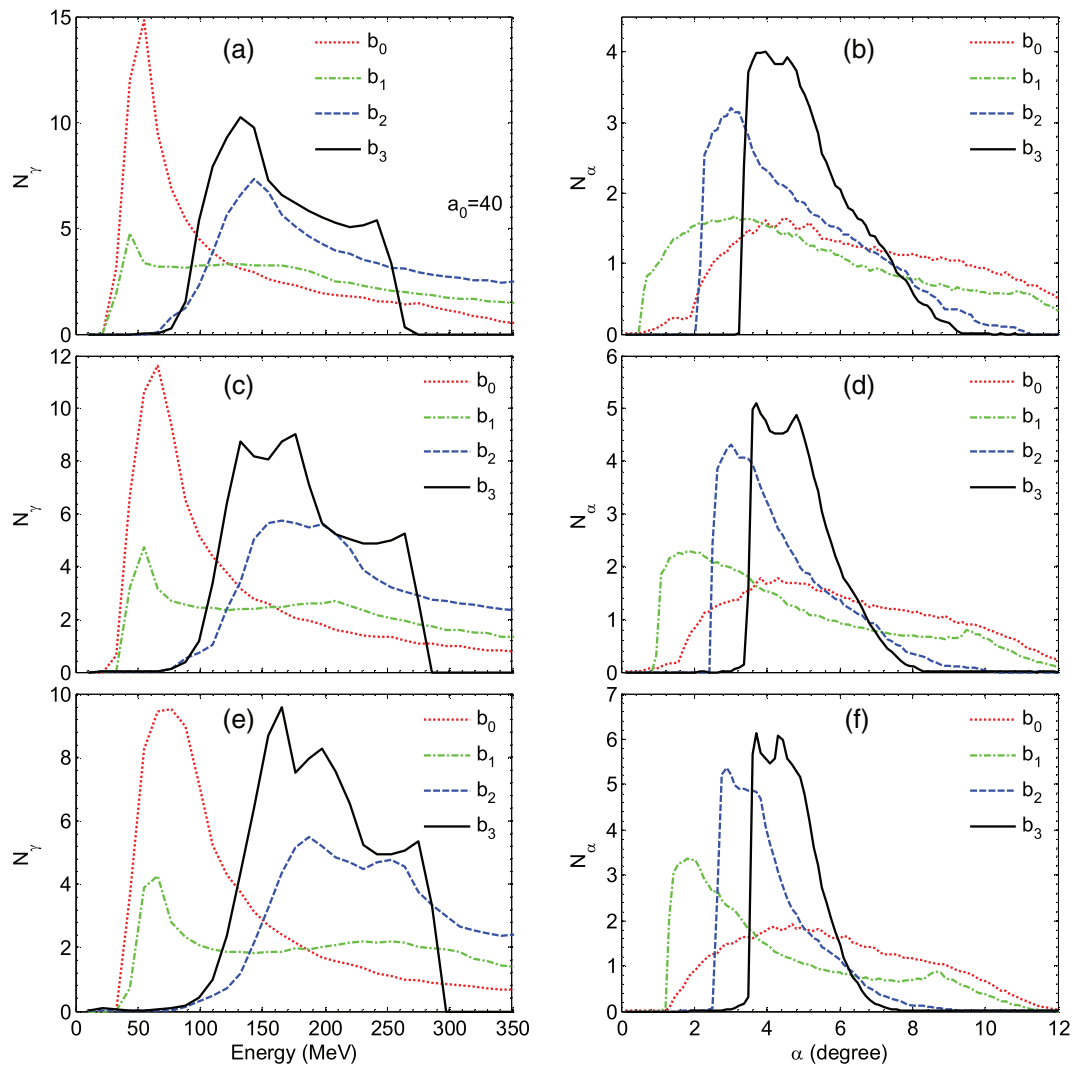


Figure 5. Spectrum of (a), (c), (e) energy and (b), (d), (f) angle of emittance of the electrons generated during the ionization of krypton ions Kr^{32+} by a circularly polarized laser pulse. The laser intensity parameters are $a_0 = 40, 50,$ and 60 for parts (a)–(f), respectively. The different colored lines are for laser frequency chirp parameters $b_0 = 0, b_1 = 10^{-4}/a_0^{0.5}, b_2 = 2 \times 10^{-4}/a_0^{0.5},$ and $b_3 = 3 \times 10^{-4}/a_0^{0.5}$.

during the ionization of krypton ions Kr^{32+} by a radially polarized laser pulse is shown in figure 4. Laser intensity parameters shown are $a_0 = 40, 50,$ and $60,$ and laser frequency chirp parameters are $b_0 = 0, b_1 = 10^{-4}/a_0^{0.5}, b_2 = 2 \times 10^{-4}/a_0^{0.5},$ and $b_3 = 3 \times 10^{-4}/a_0^{0.5}$.

The krypton ions Kr^{32+} have ionization potentials 1205.3, 2928, 3070, 3227, and 3381 for the 32th to 36th electrons, respectively. The rising part of the laser pulse is unable to ionize the krypton ions Kr^{32+} ; therefore, the electrons are released when the peak of the laser pulse interacts with the ions and gains high energy. It can be seen from the figures that the energy spectrum peak shifts towards higher energy with the introduction of the frequency chirp due to an increase in the energy of the electrons as shown in figures 1–3. The energy peaks are around 52, 63, and 38.5 MeV for the unchirped laser pulse. With the introduction of frequency chirps, the energy spectrum gets split into two peaks. The height of the peak at lower energy decreases and the height of the peak at higher energy increases with increasing frequency chirp parameters. The peak at lower energy tends to

disappear at higher values of frequency chirp parameters (for b_3). The peaks of the energy spectrum are around 147 MeV, 227 MeV, and 269 MeV for frequency chirp parameters $b_2 = 3 \times 10^{-4}/a_0^{0.5}$ for normalized laser intensity parameters $a_0 = 40, 50,$ and $60,$ respectively. It can be noted that there is an enhancement in the energy of approximately 2.8, 3.6, and 7 times with the introduction of the appropriate frequency chirp, which may be very useful for obtaining MeV electrons.

The scattering angle follows a definite relationship with the electron energy, decreasing with increasing electron energy. The scattering angle peaks are around 9.5, 7.5, and 7.4 degrees without any frequency chirp for normalized laser intensity parameters $a_0 = 40, 50,$ and $60,$ respectively. The scattering angle peaks shift to around 1.6, 2.0, and 4.0 degrees for frequency chirp parameters $b_2 = 3 \times 10^{-4}/a_0^{0.5}$ for normalized laser intensity parameters $a_0 = 40, 50,$ and $60,$ respectively. It can be noted that the scattering angle decreases for an appropriate frequency chirp, thus increasing the collimation of the electron beam.

The results of figure 4 are repeated in figure 5 for a circularly polarized laser pulse for the same parameters. The energy

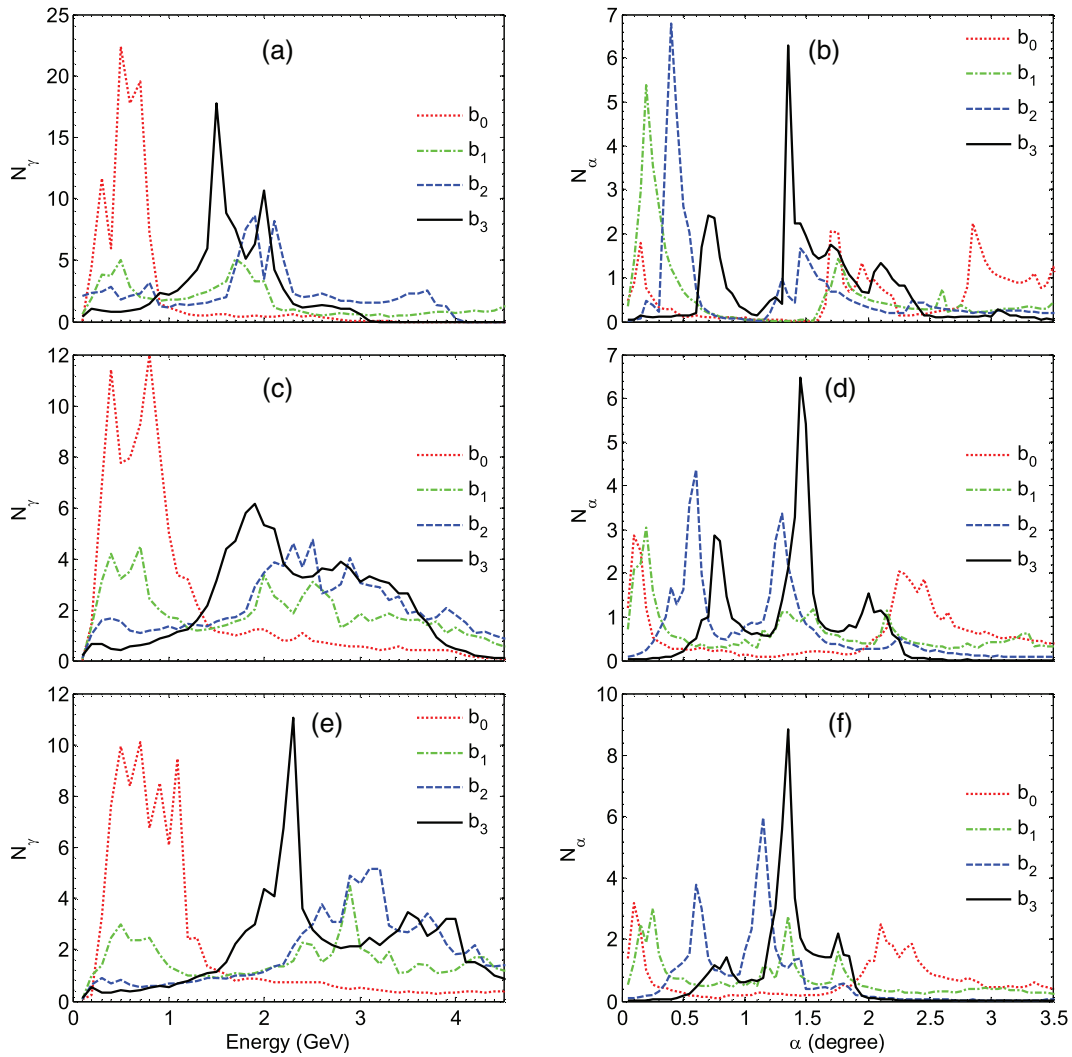


Figure 6. Spectrum of (a), (c), (e) energy and (b), (d), (f) angle of emittance of the electrons generated during the ionization of argon ions Ar^{16+} by a radially polarized laser pulse. The laser intensity parameters are $a_0 = 120, 160,$ and 200 for parts (a)–(f), respectively, and the normalized laser spot sizes are $r_0 = a_0$. The different colored lines are for laser frequency chirp parameters $b_0 = 0, b_1 = 1.5 \times 10^{-5}/a_0^{0.5}, b_2 = 3 \times 10^{-5}/a_0^{0.5},$ and $b_3 = 4.5 \times 10^{-5}/a_0^{0.5}$.

peaks are around 55 MeV, 66 MeV, and 77 MeV for unchirped laser pulses. These values are comparable to the values for the radially polarized laser pulse in figure 4. The peaks of the energy spectrum shift to around 143 MeV, 165 MeV, and 187 MeV for frequency chirp parameter $b_2 = 3 \times 10^{-4}/a_0^{0.5}$ for normalized laser intensity parameters $a_0 = 40, 50$ and 60 , respectively. It can be noted that there is an enhancement in the energy of approximately 2.6, 2.5, and 2.43 times with the introduction of the frequency chirp. The energy enhancement for the circularly polarized laser pulse is lower than that for the radially polarized laser pulse. The energy peaks are sharper for radially polarized laser pulses than for circularly polarized laser pulses.

The scattering angle peaks are around 4.44, 4.32, and 4.68 degrees without any frequency chirp for normalized laser intensity parameters $a_0 = 40, 50,$ and 60 , respectively, for circularly polarized laser pulses. These values are lower than those for radially polarized laser pulses. The scattering angle peaks shift to around 3, 3, and 2.88 degrees for frequency chirp

parameter $b_2 = 2 \times 10^{-4}/a_0^{0.5}$ for normalized laser intensity parameters $a_0 = 40, 50,$ and 60 , respectively. These values for circularly polarized pulses are higher than for radially polarized laser pulses in figure 4.

We will now discuss the acceleration of the electrons generated during the ionization of argon ions Ar^{16+} . The spectrum of energy and angle of emittance of the electrons generated during the ionization of argon ions Ar^{16+} by a laser pulse is shown in figure 6. The laser intensity parameters are $a_0 = 120, 160,$ and 200 , and the laser frequency chirp parameters are $b_0 = 0, b_1 = 1.5 \times 10^{-5}/a_0^{0.5}, b_2 = 3 \times 10^{-5}/a_0^{0.5},$ and $b_3 = 4.5 \times 10^{-5}/a_0^{0.5}$. The argon ions Ar^{16+} have ionization potentials 918.03, 4120.89, and 4426.23 for the 16th to 18th electrons, respectively. There is a significant difference between the ionization potentials of the 16th and 17th electrons which can be utilized to remove the 16 outer electrons by a prepulse. The ionization potentials are much higher than those for krypton ions, so we have to use higher laser intensity. The ions will also move in the strong field due to the

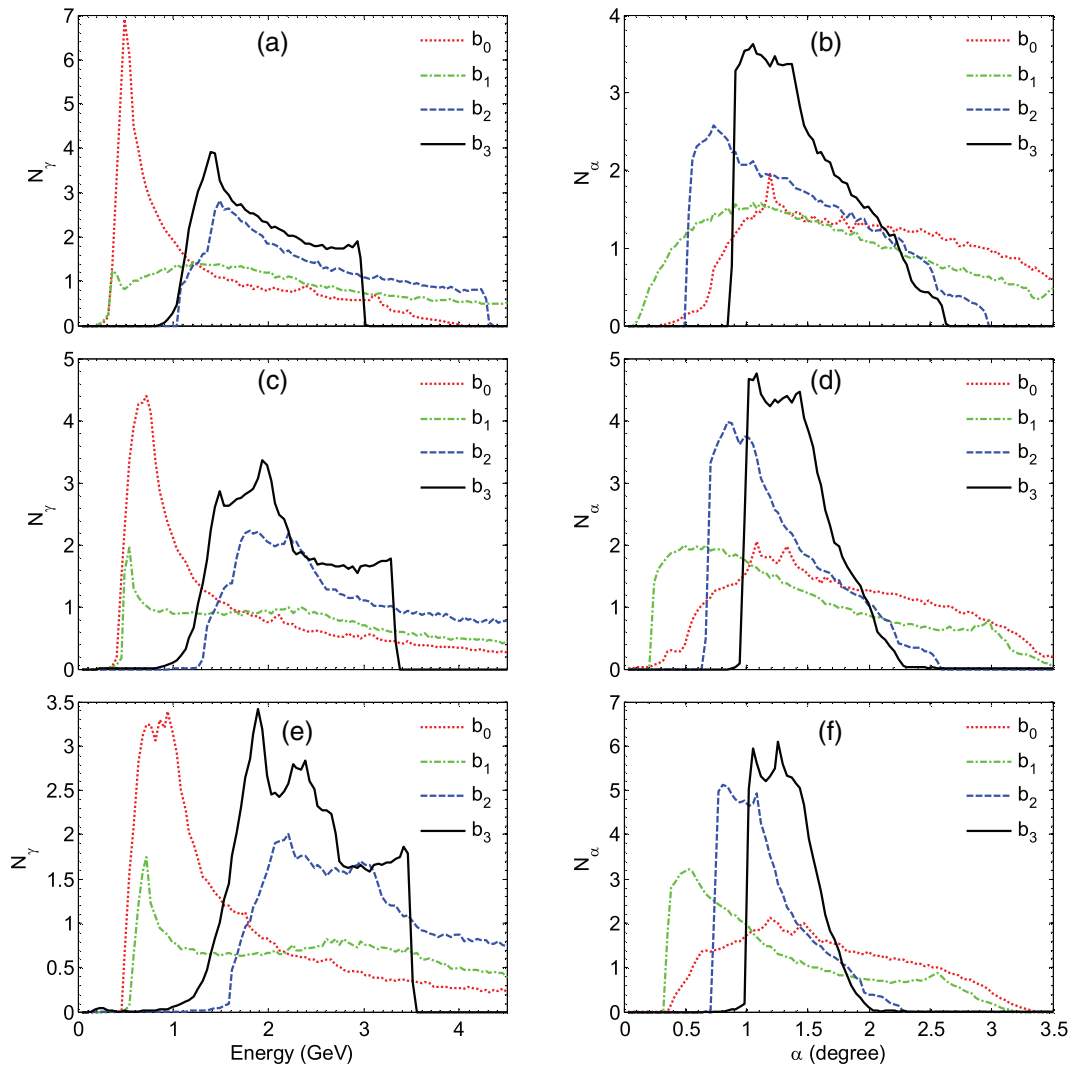


Figure 7. Spectrum of (a), (c), (e) energy and (b), (d), (f) angle of emittance of the electrons generated during the ionization of argon ions Ar^{16+} by a circularly polarized laser pulse. The laser intensity parameters are $a_0 = 120, 160,$ and 200 for parts (a)–(f), respectively, and the normalized laser spot sizes are $r_0 = a_0$. The different colored lines are for laser frequency chirp parameters $b_0 = 0, b_1 = 1.5 \times 10^{-5}/a_0^{0.5}, b_2 = 3 \times 10^{-5}/a_0^{0.5},$ and $b_3 = 4.5 \times 10^{-5}/a_0^{0.5}$.

ponderomotive potential, however, the plasma effect can be neglected due to the low gas density as stated earlier. Similar to the spectra for krypton in figure 4, the energy spectrum peak shifts towards higher energy with the introduction of a laser frequency chirp. The energy peaks are around 0.5 GeV, 0.8 GeV, and 0.7 GeV for unchirped laser pulses. Other trends in the energy and scattering spectrum are similar to those for krypton, shown in figure 4. The peaks of the energy spectrum are around 1.9, 2.5, and 3.2 GeV for frequency chirp parameter b_2 for normalized laser intensity parameters $a_0 = 120, 160$ and 200 , respectively. Again, there is an enhancement in the energy of approximately 3.8, 3.1, and 4.5 times with the introduction of the appropriate frequency chirp.

The scattering angle peaks are around 2.8, 2.25, and 2.2 degrees without any frequency chirp for normalized laser intensity parameters $a_0 = 120, 160,$ and 200 , respectively. The scattering angle peaks shift to around 0.4, 0.6, and 1.60 degrees for frequency chirp parameter b_2 . It can be noted

that the scattering angle decreases with the introduction of an appropriate frequency chirp, thus increasing collimation of the electron beam.

Obviously, the optimum value of the frequency chirp parameter decreases with laser intensity for krypton as well as argon. Magnetic focusing of the electron beam can be used to increase the charge per unit volume and collimation of the beam.

The results of figure 6 are repeated in figure 7 for a circularly polarized laser pulse for the same parameters. The energy peaks are around 0.5 GeV, 0.72 GeV, and 0.95 GeV for unchirped circularly polarized laser pulses, which is comparable to those for radially polarized laser pulses. The peaks of the energy spectrum are around 1.49 GeV, 1.8 GeV, and 2.2 GeV for circularly polarized laser pulses for frequency chirp parameter b_2 for normalized laser intensity parameters $a_0 = 120, 160,$ and 200 , respectively. There is an enhancement in the energy of approximately 3, 2.5, and 2.3 times

with the introduction of a frequency chirp. From the comparison of the above results, it can be noted that the energy enhancement with the introduction of a frequency chirp is not as high for circularly polarized laser pulses as for radially polarized pulses.

The energy peaks are sharper for radially polarized laser pulses than for circularly polarized laser pulses, which implies that the electron beam is more monoenergetic for radially polarized pulses.

The scattering angle peaks are around 1.19, 1.08, and 1.19 degrees without any frequency chirp for normalized laser intensity parameters $a_0 = 120, 160, \text{ and } 200$, respectively. These values are around half as high as the values found for radially polarized laser pulses. The scattering angle peaks shift to around 0.73, 0.84, and 0.81 degrees for frequency chirp parameter b_2 . These values are comparable to those for radially polarized laser pulses.

If we look at the results for the circularly polarized cases (figures 5 and 7) we find that the energy is highest for chirp parameter b_2 . So the value of frequency chirp b_2 is optimized for circularly polarized laser pulses.

Conclusion

To summarize, we have investigated the energy enhancement of electrons generated during the ionization of low-density krypton ions Kr^{32+} and argon ions Ar^{16+} by a radially polarized laser pulse using a negative frequency chirp. There exists an optimum value of laser spot size and frequency chirp for which the electron energy is at its maximum. The energy of the electrons can be increased and scattering can be decreased using an optimum frequency chirp. The optimum value of the frequency chirp decreases with laser intensity and as well as spot size. The electron energy strongly depends upon initial time t_0 . The chirped radially polarized laser pulse is more efficient than the chirped circularly polarized laser pulse at enhancing energy and obtaining quasi-monoenergetic electron beams. The proposed scheme can be used to obtain quasi-monoenergetic collimated MeV/GeV electrons.

Acknowledgments

This work was supported and the acceleration simulation code used in this work was developed by Singh Simutech Pvt. Ltd., Bharatpur, Rajasthan, India.

References

- [1] Perry M D and Mourou G 1994 *Science* **264** 917
- [2] Joshi C J and Corkum P B 1995 *Phys. Today* **48** 36
- [3] Esarey E, Sprangle P, Krall J and Ting A 1996 *IEEE Trans. Plasma Sci.* **24** 252
- [4] Modena A et al 1995 *Nature* **377** 606
- [5] Leemans W P, Nagler B, Gonsalves A J, Toth Cs, Nakamura K, Geddes C G R, Esarey E, Schroeder C B and Hooker S M 2006 *Nat. Phys.* **2** 696
- [6] Amendt P, Eder D C and Wilks S C 1991 *Phys. Rev. Lett.* **66** 2589
- [7] Esarey E, Ride S K and Sprangle P 1993 *Phys. Rev. E* **48** 3003
- [8] Tabak M, Hammer J, Glinzky M E, Kruer W L, Wilks S C, Woodworth J, Campbell E M, Perry M D and Mason R J 1994 *Phys. Plasmas* **1** 1626
- [9] Khachatryan A G, van Goor F A and Boller K-J 2004 *Phys. Rev. E* **70** 067601
- [10] Singh K P 2005 *Appl. Phys. Lett.* **87** 254102
- [11] Gupta D N and Suk H 2007 *Laser Part. Beams* **25** 31
- [12] Sohbatzadeh F, Mirzanejhad S and Ghasemi M 2006 *Phys. Plasmas* **13** 123108
- [13] Gupta D N, Hur M S and Suk H 2007 *Phys. Plasmas* **14** 044701
- [14] Gupta D N, Jang H J and Suk H 2009 *J. Appl. Phys.* **105** 106110
- [15] Singh K P and Sajal V 2009 *Phys. Plasmas* **16** 043113
- [16] Sohbatzadeh F, Mirzanejhad S, Aku H and Ashouri S 2010 *Phys. Plasmas* **17** 083108
- [17] Li J-X, Zang W-P and Tian J-G 2010 *Appl. Phys. Lett.* **96** 031103
- [18] Song Q, Wu X Y, Wang J X, Kawata J X and Wang P X 2014 *Phys. Plasmas* **21** 054503
- [19] Salamin Y I and Jisrawi N M 2014 *J. Phys. B: At. Mol. Opt. Phys.* **47** 025601
- [20] Singh K P and Kumar M 2011 *Phys. Rev. ST Accel. Beams* **14** 030401
- [21] Singh K P, Sajal V and Gupta D N 2008 *Laser Part. Beams* **26** 597
- [22] Moore C I, Ting A, Jones A, Briscoe A, Hafizi B, Hubbard R F and Sprangle P 2001 *Phys. Plasmas* **8** 2481
- [23] Singh K P, Arya R and Malik A K 2015 *Phys. Plasmas* **22** 083105